rsta.royalsocietypublishing.org Phil. Trans. R. Soc. A 20190341

Variability in Electrophysiological Properties and Conducting Obstacles Controls Re-entry Risk in Heterogeneous Ischaemic Tissue – Supplementary Material

Brodie A. J. Lawson, Rafael S. Oliveira, Lucas A. Berg,
Pedro A. A. Silva, Kevin Burrage, Rodrigo Weber dos Santos

Supplementary Figures

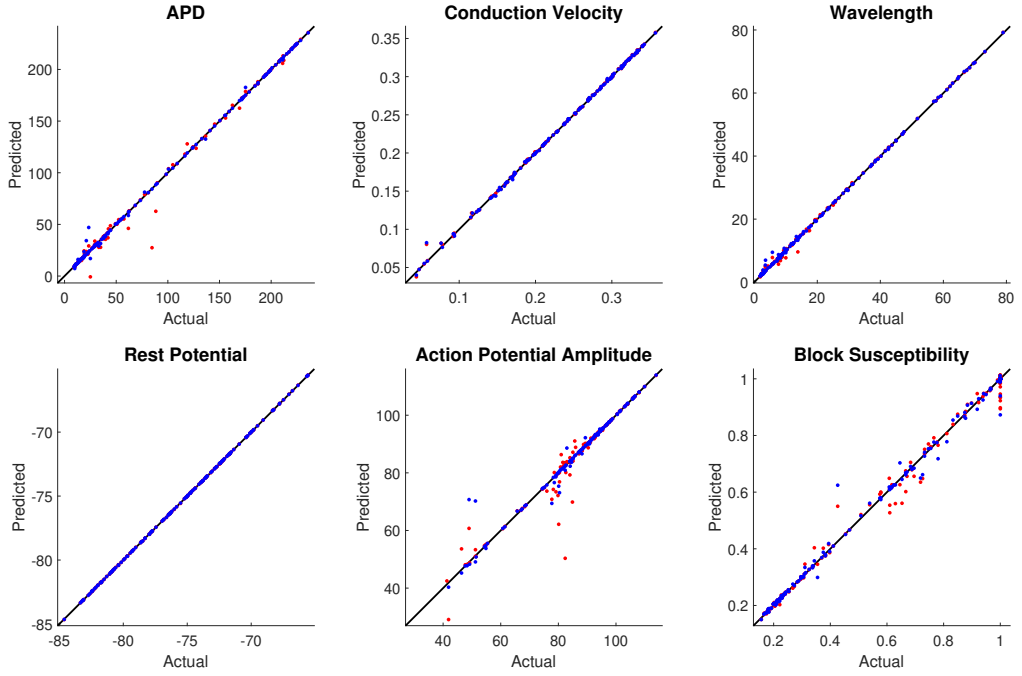

Figure S1. Performance of partitioned emulation for the different qualities of interest. Visualised are the predicted and actual values for the test data, unseen during emulator construction, using regular (red) or partitioned (blue) emulation. Lines of equality are shown in black. Partitioned emulators show very good performance, with almost all predictions falling very close to the line of equality. Those that are less well predicted are due to being assigned to the incorrect partition by the support vector machine classifier. Regular emulation shows good, but inferior, performance, and in fact struggles further than implied by the figure due to generating wild predictions in regions where the quantity of interest cannot be measured (which are correctly separated out by partitioning).

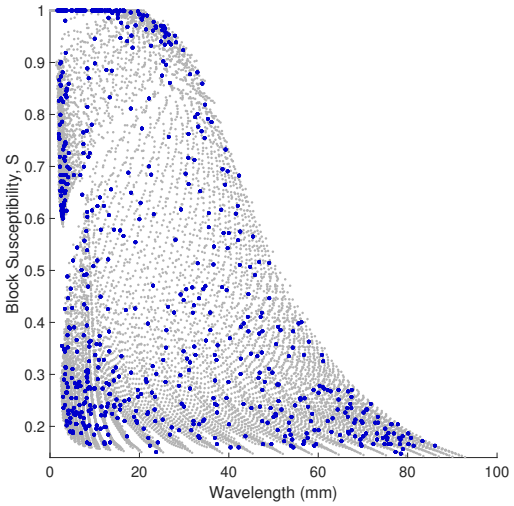

Figure S2. Partitioned emulation successfully predicts the dependence of the two most important quantities of interest on one another. Data points collected from simulations in tissue fibres (blue) show clear, but nonlinear dependence between action potential wavelength and block susceptibility, S. The emulator's predictions throughout the parameter space (grey) demonstrate all of the same trends.

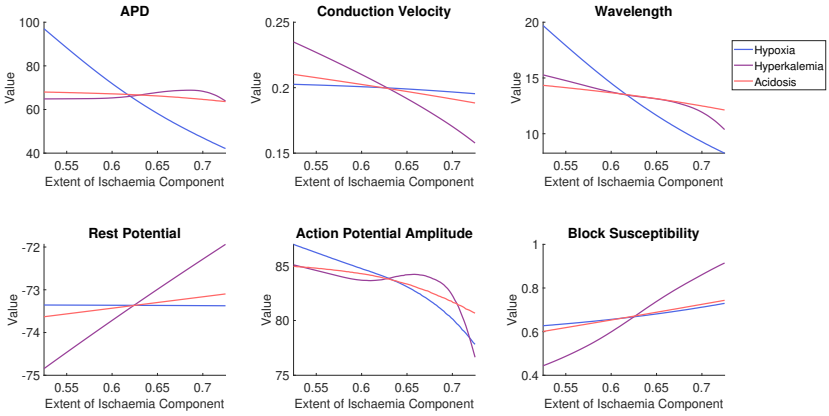

Figure S3. Main effects of ischaemia components on excitation propagation in a tissue fibre, over a range regarding intermediate progression of the condition. Trends in the quantities of interest match those shown by the main effects over the full parameter space, save for a minor positive effect of hyperkalemia on action potential duration (due to the shifted equilibrium potential for K^+ weakening repolarising currents). This also results in a complex dependence of the action potential amplitude on hyperkalemia, before weakened excitation due to the depolarised rest potential dominates as hyperkalemia extent increases further.

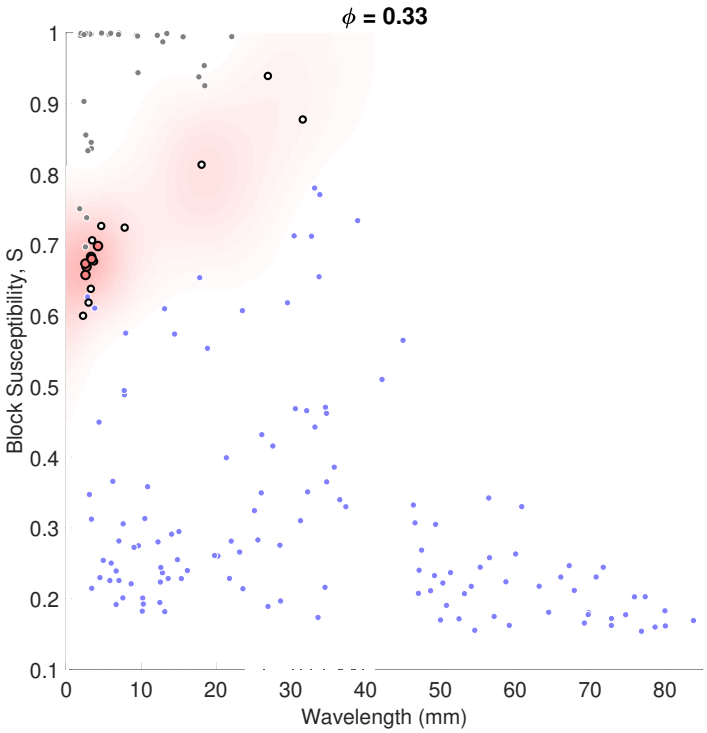

Figure S4. Smooth maps of risk created to estimate risk away from observed data. Depth of red indicates the extent of risk of re-entry. Dots indicate observations from 2D tissue simulations, including failure to propagate (grey), propagation without re-entry (blue), local re-entry (white) and transient and sustained re-entry (red).

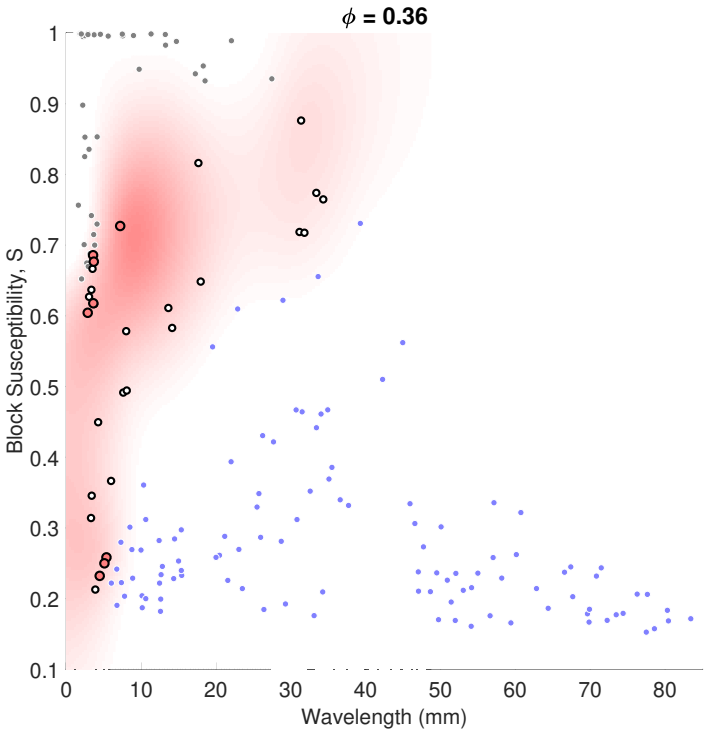

Figure S5. Smooth maps of risk created to estimate risk away from observed data. Depth of red indicates the extent of risk of re-entry. Dots indicate observations from 2D tissue simulations, including failure to propagate (grey), propagation without re-entry (blue), local re-entry (white) and transient and sustained re-entry (red).

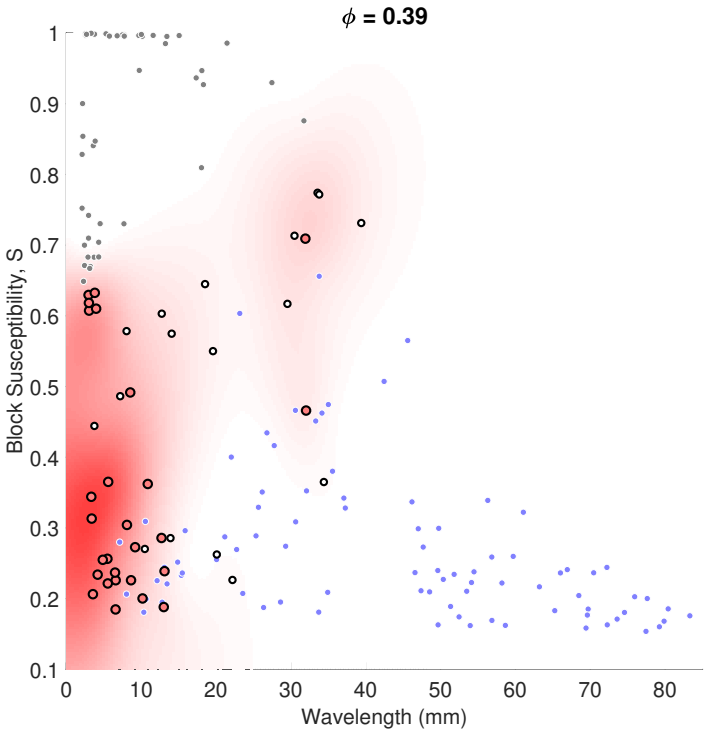

Figure S6. Smooth maps of risk created to estimate risk away from observed data. Depth of red indicates the extent of risk of re-entry. Dots indicate observations from 2D tissue simulations, including failure to propagate (grey), propagation without re-entry (blue), local re-entry (white) and transient and sustained re-entry (red).

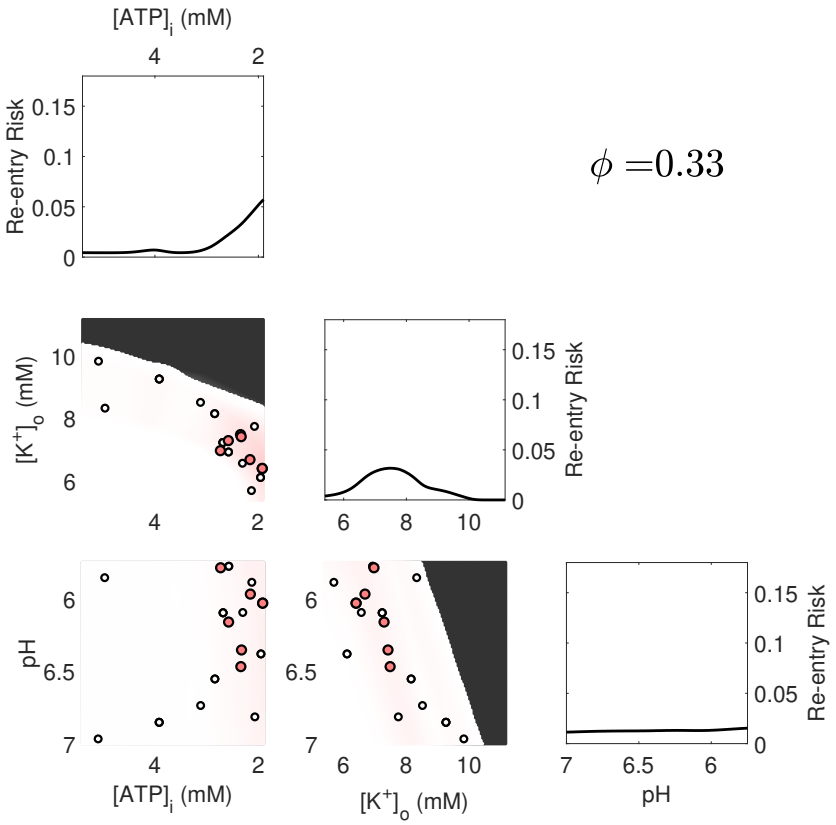

Figure S7. Manifestations of ischaemic remodelling with the potential for re-entry. Marginal distributions show the result of integrating over variation in the remaining two parameters. Depth of red indicates the extent of risk of re-entry. Dark grey regions mark regions predicted to block (with insignificant risk of re-entry). For reference, the 2D simulation data showing local re-entry (white) or transient or sustained re-entry (red) is projected onto the same parameter space.

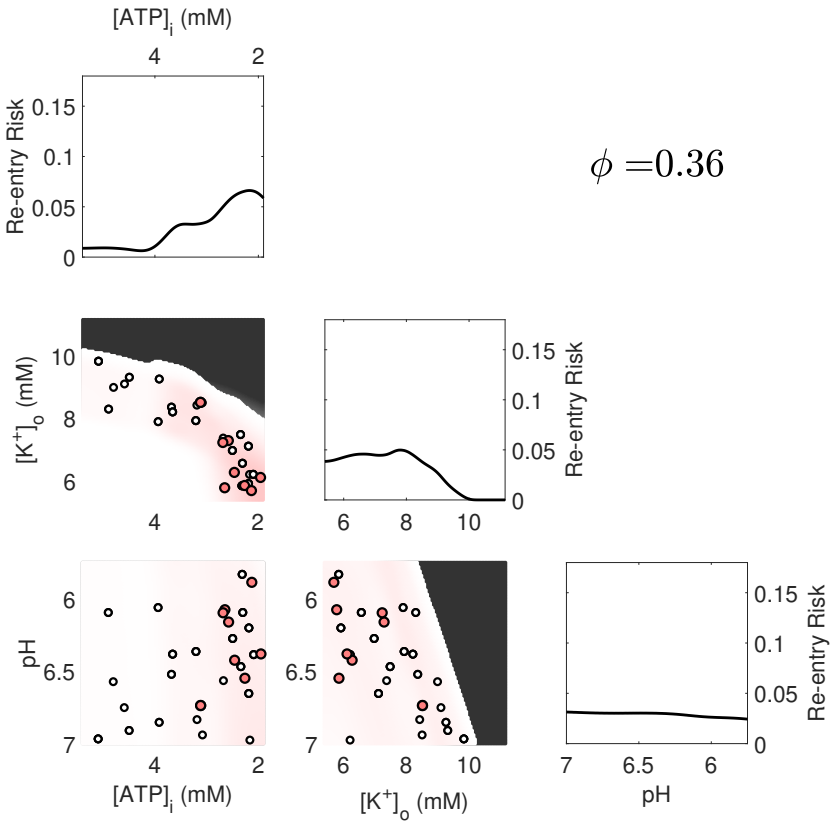

Figure S8. Manifestations of ischaemic remodelling with the potential for re-entry. Marginal distributions show the result of integrating over variation in the remaining two parameters. Depth of red indicates the extent of risk of re-entry. Dark grey regions mark regions predicted to block (with insignificant risk of re-entry). For reference, the 2D simulation data showing local re-entry (white) or transient or sustained re-entry (red) is projected onto the same parameter space.

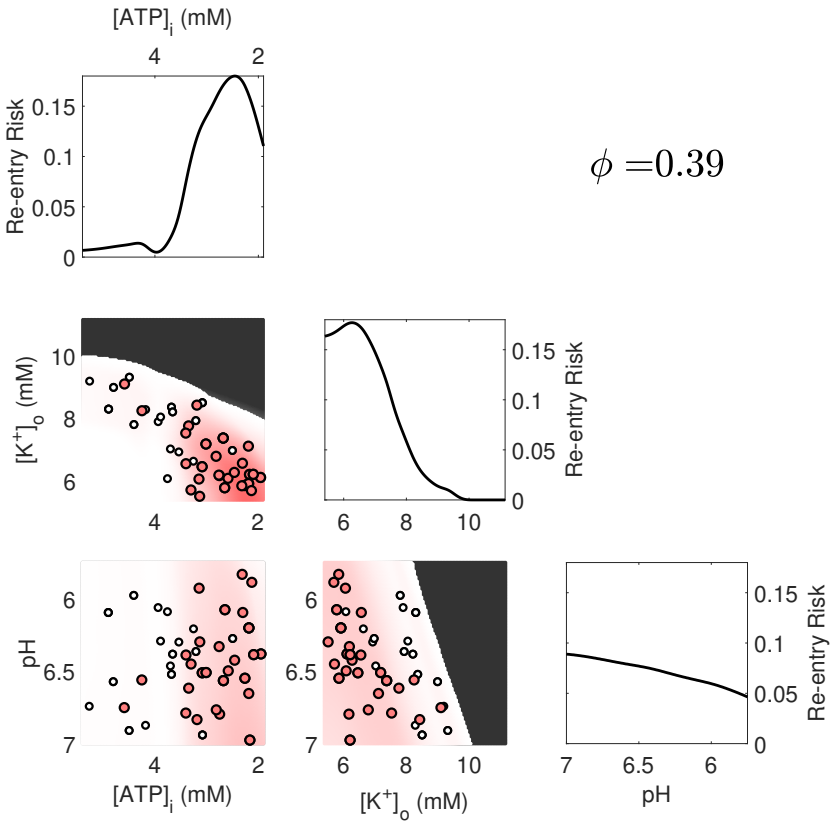

Figure S9. Manifestations of ischaemic remodelling with the potential for re-entry. Marginal distributions show the result of integrating over variation in the remaining two parameters. Depth of red indicates the extent of risk of re-entry. Dark grey regions mark regions predicted to block (with insignificant risk of re-entry). For reference, the 2D simulation data showing local re-entry (white) or transient or sustained re-entry (red) is projected onto the same parameter space.

Gaussian Process Methodology

Generating Emulator Predictions

The main document details how partitioning is used to improve emulation, but this section provides further information regarding the basic Gaussian process (GP) methodology. Here, as in the main document, inputs to a model are denoted $\boldsymbol{\theta}$ and its m-th output is denoted y_m. The training data is then a matrix of input values (each row a set of parameters $\boldsymbol{\theta}$), $\boldsymbol{\Theta}$, and a corresponding vector of values for an output quantity of interest, $\mathbf{y}_m$.

First, a best-fit linear trend is subtracted from the data, so that the GP is then attempting to non-parametrically fit the remaining residuals. That is, the training data's model outputs are transformed according to

$$\mathbf{z}_m = \mathbf{y}_m - \mathbf{X}\left(\mathbf{X}^T\mathbf{X}\right)^{-1}\mathbf{X}^T\mathbf{y}_m, \qquad \mathbf{X} = [\mathbf{1}, \boldsymbol{\Theta}].$$

A zero-mean GP, which is defined entirely by its covariance function $k = (\boldsymbol{\theta}, \boldsymbol{\theta}'; \boldsymbol{\phi})$, is then fit to this transformed data. Fitting here refers to selection of the hyperparameters $\boldsymbol{\phi}$ by maximising the likelihood that the data would be generated by a GP with those hyperparameters, which has an analytical form,

$$\boldsymbol{\phi}_{\text{MLE}} = \arg\max_{\boldsymbol{\phi}}\left(-\mathbf{z}_m^T\left[\mathbf{K}(\boldsymbol{\phi})\right]^{-1}\mathbf{z}_m - \ln\det\mathbf{K}(\boldsymbol{\phi})\right).$$

Here $\mathbf{K}(\boldsymbol{\phi})$ is the covariance matrix between all of the input training points, with elements given by $K_{ij}(\boldsymbol{\phi}) = k(\boldsymbol{\Theta}_{i*}, \boldsymbol{\Theta}_{j*}; \boldsymbol{\phi})$ and subscript $_{i*}$ denoting the i-th row of the matrix. The first term of this likelihood represents the goodness of data fit, and the second the complexity of the fitted surface, and as such maximising the likelihood represents compromising between the two (helping decrease the risk of overfitting).

This work uses the automatic relevance determination variation of the Matern-3/2 covariance function, defined

$$k(\boldsymbol{\theta}, \boldsymbol{\theta}'; \boldsymbol{\phi}) = \sigma^2(1+\sqrt{3}r)\exp -\sqrt{3}r + \sigma_n^2\delta_{\boldsymbol{\theta},\boldsymbol{\theta}'}, \qquad r = \sqrt{\sum_{d=1}^{N_{\text{params}}}\frac{(\theta_d - \theta_d')^2}{l_d^2}},$$

with θ_d denoting the value of the d-th parameter in $\boldsymbol{\theta}$ (and similarly for θ'), $\delta_{x,y}$ the Kronecker delta and $\boldsymbol{\phi} = (\mathbf{l}, \sigma, \sigma_n)$ the hyperparameters consisting of effect lengths for each parameter, overall variance, and noise in the process, respectively.

With a GP trained (selecting $\mathbf{K}_{\text{MLE}} = \mathbf{K}(\boldsymbol{\phi}_{\text{MLE}})$), a prediction at a point $\boldsymbol{\theta}$ can then be made using the mean of the process,

$$z_{j,\text{pred}}(\boldsymbol{\theta}) = \mathbf{K}_{\text{MLE}}^*\mathbf{K}_{\text{MLE}}^{-1}\mathbf{z}_m, \qquad (\mathbf{K}_{\text{MLE}}^*)_i = k(\boldsymbol{\theta}, \boldsymbol{\Theta}_{i*}; \boldsymbol{\phi}_{\text{MLE}}).$$

Prediction for the actual output quantities is then completed by combining the best linear fit with the predicted residual away from that linear fit,

$$y_{j,\text{pred}}(\boldsymbol{\theta}) = \boldsymbol{\theta}\left(\mathbf{X}^T\mathbf{X}\right)^{-1}\mathbf{X}^T\mathbf{y}_m + \mathbf{K}_{\text{MLE}}^*\mathbf{K}_{\text{MLE}}^{-1}\mathbf{z}_m.$$

Note that here (and in the above), $\boldsymbol{\theta}$ is treated as a row vector.

Risk Surface Construction

For constructing a risk surface (used to generate Figure 8 in the main document), a GP was used as a way to estimate risk away from the data collected from simulations in two-dimensional heterogeneous tissue. Risk was calculated by averaging over the three simulations performed for each combination of parameter and ϕ values, an insufficient sample to correctly estimate the true proportion of realisations of heterogeneity that will exhibit re-entry. As such, this GP was used simply as a compelling option for producing a smoothed surface of risk that reflected in some sense the uncertainty in the true risk away from the collected data, including a contribution towards lower risk from "negative" data (observations of no re-entry).

The tissue simulations were used to estimate Risk according to

$$R_{jk} = R(\mathbf{m}_j, \phi_k) = \frac{1}{3} \sum_{n=1}^{3} \left(\mathbb{1}_{C_i(\mathbf{m}_j,\phi_k)=\text{re-entry}} + 0.2\, \mathbb{1}_{C_i(\mathbf{m}_j,\phi_k)=\text{local}} \right).$$

Recalling that risk estimation is carried out in the "metric" space (WL,S) so that the smoothing implies similar *dynamics* will present similar risk (instead of just similar values of *parameters*), the "parameters" here are the vectors of metrics $\mathbf{m} = (\text{WL}, S)$. $C_i(\mathbf{m}_j, \phi_k)$ is the class of behaviour observed for the i-th simulation using parameters that gave metrics $\mathbf{m}_j$ in the tissue fibre simulations, and obstacle proportion ϕ_k. The formula corresponds to assigning a risk of unity to simulations showing "re-entry" (transient or sustained), and 20% as much risk to simulations that showed local re-entry (see Table 2 in main document). Other simulations (whether successfully propagating or not) were assigned zero risk.

Surfaces were constructed using the risk data directly (no transformation first removing a parametric trend). Each proportion of obstacles was treated separately, providing estimated risk at any point in the parameter space for a given ϕ_k according to

$$R_{\text{pred}}(\mathbf{m}, \phi_k) = \mathbf{K}_R^*(\mathbf{m})\, \mathbf{K}_R^{-1} R_{*k}.$$

Here $\mathbf{K}_R$ and $\mathbf{K}_R^*$ are covariance matrices defined in the same manner as above, but with hyperparameters specified to attain a desired level of smoothing,

$$l_{\text{WL}} = 2.5, \qquad l_S = 0.2, \qquad \sigma = 0.2, \qquad \sigma_n = 0.1.$$